

# Identification of fNIRS based Brain Activity using Adaptive Algorithm

M. Ahmad Kamran, Keum-Shik Hong, Malik M. Naeem Mannan

Department of Cogno-Mechatronics Engineering  
 School of Mechanical Engineering  
 Pusan National University, Busan, Korea  
 {malik, kshong}@pusan.ac.kr  
 Department of Cogno-Mechatronics Engineering  
 Pusan National University, Busan, Korea  
 uetmathematics@yahoo.com

## Abstract

Functional near infrared spectroscopy (fNIRS) is non-invasive brain imaging techniques that detects the cortical activity by measuring the change in the concentration of oxy-hemoglobin and de-oxy hemoglobin. It uses near infrared light of two wave lengths, 760 nm and 830 nm. NIRS is emerging neuro imaging modality with high temporal resolution. The advantage of NIRS system over other neuro imaging modalities is low cost, portable, safe and somehow results in short period of time. The scalp remains intact throughout the experiment. In this study we present a method for identification of brain activity by using fNIRS data. The general linear model has been used in study with predicted blood oxygen level dependent (BOLD) response signal and its delayed versions. The normalized least mean square (NLMS) algorithm has been used for identification of unknown parameters in the model recursively. A one way t-test has been performed for the significance of results.

**Keywords:** General linear model (GLM), blood oxygen level dependent, normalized least mean square algorithm, adaptive filtering.

## Introduction

There are several non-invasive neuro imaging techniques available at the moment e.g., electroencephalography (EEG), positron emission tomography (PET), magnetoencephalography (MEG), single photon emission computed tomography (SPECT), and functional magnetic resonance imaging (fMRI) etc. MEG and EEG provide direct information about neuronal activity [1]. The basic principle of EEG is to measure electric field caused by cortical activity and MEG measures the magnetic field induced by the neuronal activity. PET, SPECT and fMRI are the indirect methods to measure brain activity. The magnetic field caused by fMRI machine gives information about the change in de-oxy hemoglobin, while PET and SPECT use the decay of radioactive isotopes. Jobsis [2] for the first time discovered that information about neuronal activity can be measured by applying laser light to scalp.

Near infrared spectroscopy (NIRS) method is non-invasive brain imaging technique which measures the activity of brain using near infrared light of 650 nm to 950 nm wavelengths [1, 3, 4, and 5]. fNIRS detects the change in the concentration of oxy hemoglobin and de-oxy hemoglobin depending on the scattering/absorption of near infrared light which passes through scalp and absorbed/scattered in brain tissue. fNIRS has great potential for brain activity measurement as fNIRS system is compact, portable and inexpensive. It has very high temporal resolution [3] and it can be safely used for detecting cortical development or activity in children/infants as well as adults [6].

In past, information about brain activity was gathered by using two steps procedure. The first step involves the collection of data while other includes the offline analysis/processing [7]. The recent research shows great

potential in fNIRS based brain computer interface (BCI) [8]. fNIRS based real time BCI have been reported in [7, 9, and 10]. fNIRS signal is highly sensitive to hemodynamic fluctuations, which is biggest challenge for researcher working in the field of optical tomography. This sensitivity due to hemodynamic fluctuation depends on the source-detector distance [11], which is deciding factor for the banana shape path of near infrared light inside the scalp.

General linear model has been most commonly used tool for the analysis of fMRI data [12]. Schrooter and Bucheler were one of the first groups who used GLM for fNIRS data [13]. The basic idea of GLM is to use visual stimuli and hemodynamic response function (HRF) to separate out the predicted the blood oxygen level dependent (BOLD) response from the fNIRS signal. The HRF function is composed of two gamma functions. There are many commonly used systems in the world which are nonlinear in behavior and brain is an example of the most complex nonlinear system. The system identification of such non-linear systems is the topic of research of many research groups. fNIRS gives the information about the change in concentration of chromospheres at discrete steps of time. The input-output dynamic model of such discrete system with unknown input is a difficult task. Most of the research group's use predicted BOLD response as the output for brain activity which is the convolution of HRF and experimental paradigm. The indirect input for generating brain activity at particular area of brain is visual stimuli. In this study we have presented a technique for identification of predicted BOLD response from hemodynamic response recorded using fNIRS by generating cortical activity in left motor cortex using right hand finger tapping task. The unknown parameters involved in GLM are estimated by using normalized least mean square algorithm.

This paper has been divided into three sections. First section describes the detail of material and methods, second section is reserved for experimental paradigm and data acquisition, and third section has results and conclusion.

## Materials and Methods

In this section, we will describe the basic idea of GLM for the analysis of fNIRS data and normalized least mean square algorithm for recursive estimation of unknown parameters of general linear model.

### A. General Linear Model (GLM)

The sum of linear combination of known regressor and Gaussian noise can represent the data variable of NIRS system, which is the basic theme of GLM. Mathematically, let  $y^i \in R^N$  represent the change of concentration of oxy-hemoglobin or de-oxy hemoglobin and  $\varepsilon^i \in R^n$  is the Gaussian noise with zero mean, then corresponding GLM model is given by

$$y^i = [y^i(t_1) \ y^i(t_2) \ y^i(t_3) \dots \dots y^i(t_N)], \quad (1)$$

$$\varepsilon^i = [\varepsilon^i(t_1) \ \varepsilon^i(t_2) \ \varepsilon^i(t_3) \dots \dots \varepsilon^i(t_N)], \quad (2)$$

$$y^i = X\beta^i + \varepsilon^i, \quad (3)$$

where  $X \in R^{N \times M}$  is known as design matrix and  $\beta^i \in R^{M \times 1}$  is the corresponding response signal strength  $i$ th channel.

The design matrix contains the predicted BOLD response and its derivatives. The predicted BOLD response is the convolution of HRF and experimental paradigm, described in Section III. The unknown parameters, the response signal strength  $\beta^i \in R^{M \times 1}$  of can be optimized using ordinary least square method as

$$\hat{\beta}^i = (X^T X)^{-1} X^T y^i. \quad (4)$$

In this study, we use design matrix to be composed of predicted BOLD response function and its delayed version at each time step. The values of unknown parameters have been estimated by using normalized least mean square (NLMS) algorithm recursively. Under the null hypothesis,  $c^T \beta^i = 0$  where  $c$  is a contrast vector, the corresponding  $t$ -values have been calculated for validation of results.

$$t = \frac{c^T \hat{\beta}^i}{SD(c^T \hat{\beta}^i)} \quad (5)$$

### B. Normalized Least Mean Square Algorithm

Adaptive filters with least mean square (LMS) adaptation mechanism has widely been used in field of controls, communications, signal and image processing. The LMS algorithms have two main processing steps. The first step is to get the error signal by comparing the output of a filter to certain input and some desired response. The other steps involve the up gradation of filter parameters on the basis of error [14]. The problem of gradient noise amplification due to large input is the main cause of switching from LMS to NLMS. Mathematically, let the input vector  $g(k)$  produces an output signal of the filter represented by  $\hat{d}(k)$  which is

subtracted from desired response  $y(k)$  to generate the error signal  $e(k)$ . Let us assume  $\hat{\beta}(k)$  and  $\beta(k)$  are weight vectors at two adjacent time steps. Then,

$$\hat{\beta}(k+1) = \hat{\beta}(k) + P(k)e(k), \quad (6)$$

$$P(k) = \frac{\mu g(k)}{\|g(k)\|^2}, \quad (7)$$

where  $\mu$  is the adaptation constant.

## Experimental Setup

This section has the detail information about experimental setup. First the information of experimental paradigm is described and after that data acquisition and preprocessing have been discussed in detail.

### A. Experimental Paradigm

fNIRS experimental data were recorded from five volunteers (male) age between 25 to 35. None of the subject was having neurological disorder history. Also none of the subject was taking any medication at time of experiment. The experiments were performed using continuous wave NIRS system (DYNOT: Dynamic Near Infrared Optical Tomography made by NIRx medical technologies, Brooklyn, NY) at a sampling rate of 1.81 Hz. We used near infrared light of 760 nm and 830 nm wavelengths. The distance between source and detector was 2.5 cm. The data were recorded from left motor cortex as subjects were performing right hand finger tapping. Each experiment started with 60 second preparation (discarded) followed by 40 seconds session in which 20 second rest and 20 second task. The experimental paradigm is shown in Fig. 1 and the source detector configuration and channel position is shown in Fig. 2.

### B. Data Aquisition

The change in concentration of oxy-hemoglobin (HbO) and de-oxy hemoglobin (HbR) due to neuronal activation can be measured using modified Beer Lambert law (MBLL).

Mathematically, the optical density variation  $\Delta \phi(r, s; \lambda, t)$  at a particular time  $t$  due to the change in the concentration of

$$\Delta \phi(r, s; \lambda, t) = - \ln \frac{I_{out}(r, s; \lambda, t)}{I_{in}(r, s; \lambda)} \quad (8)$$



Figure 1: Experimental paradigm

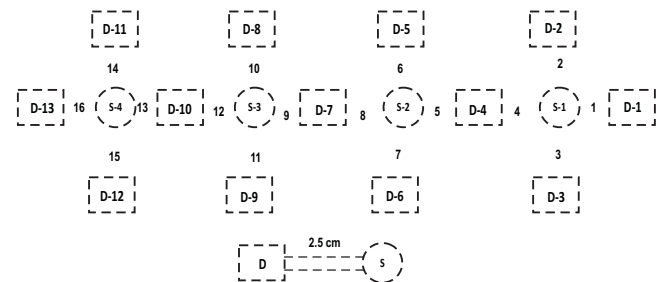


Figure 2: The channel configuration

HbO and HbR [3, 15] is described by the following MBLL.

$$\Delta\phi(r, s; \lambda, t) = [a_{HbO}(\lambda) \quad a_{HbR}(\lambda)] \begin{bmatrix} \Delta c_{HbO}(r; t) \\ \Delta c_{HbR}(r; t) \end{bmatrix} d(r)l(r) \quad (9)$$

where  $\lambda$  is the wavelength  $I_{out}(r, s; \lambda, t)$  is the photon flux at any time instant  $t$ ,  $I_{in}(r, s; \lambda)$  is the photon flux at initial time  $t = 0$ , is the source-detector position,  $l(r)$  is the source-detector distance,  $d(r)$  is the differential path length factor, and  $a_{HbO}(\lambda)$  and  $a_{HbR}(\lambda)$  are the extinction coefficients of HbO and HbR. According to MBLL, the optical density of two laser source can be used to estimate total oxy-hemoglobin (HbX) as follows.

$$\begin{bmatrix} \Delta\phi_{HbO}^i(t) \\ \Delta\phi_{HbR}^i(t) \end{bmatrix} = \begin{bmatrix} a_{HbO}(\lambda_1) & a_{HbR}(\lambda_1) \\ a_{HbO}(\lambda_2) & a_{HbR}(\lambda_2) \end{bmatrix}^{-1} \begin{bmatrix} \Delta\phi^i(t, \lambda_1) \\ \Delta\phi^i(t, \lambda_2) \end{bmatrix} \quad (10)$$

## Conclusions

A wide range of signal processing applications are dependent on adaptive system identification. The identification of neuronal activity at particular time instant is really a challenging task due to many physiological noises that occur in the signal. Adaptive algorithms somehow give good idea about the characteristics of neuronal activity among existing methods. The method presented in this study is an extension of GLM analysis with use of delayed Predicted BOLD response and use of adaptive filtering algorithm, NLMS, for estimation of unknown parameter of the model. The basic GLM uses the predicted BOLD response and its derivative as regressors.

The input stimuli shown in Fig. 3 (top) identify the rest and task session. The magnitude zero and one correspond to the rest and the task, respectively. The HRF shown in Fig. 3 (middle) can be defined by using five parameters, namely, magnitude of initial dip, time to reach main peak, magnitude of main peak, magnitude of undershoot, and time taken to reach undershoot peak from main peak. The predicted BOLD response is shown in Fig. 3 (bottom), which is the convolution of input stimuli and HRF.

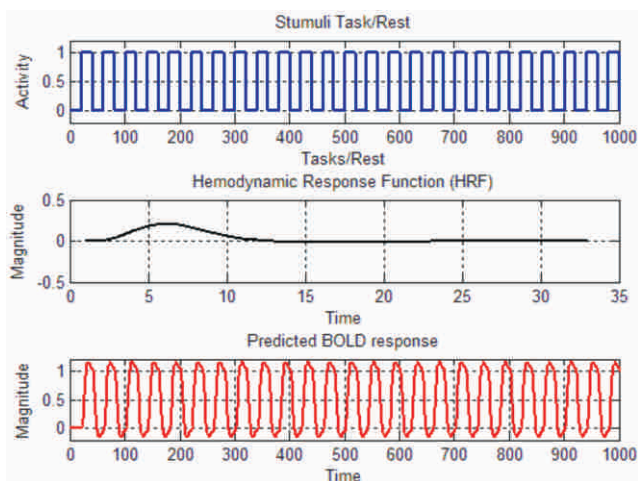


**Figure 3: Input and predicted output signals**

The estimated BOLD hemodynamic response has been shown in Fig.4. The estimate of predicted BOLD response of one

active channel and one deactivate channel has been shown in Fig. 4 and Fig. 5 respectively.

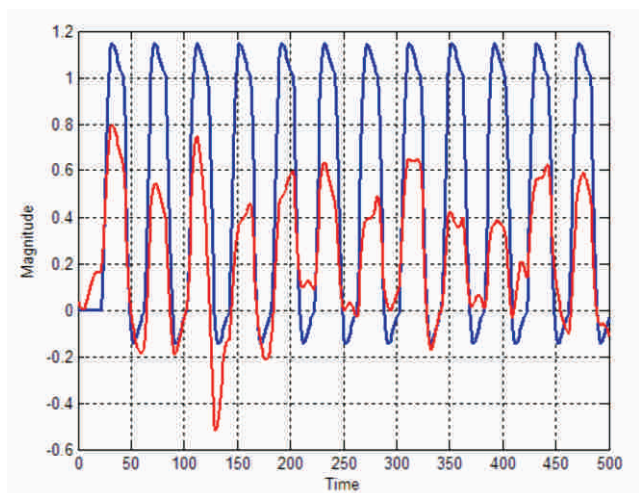


**Figure 4: The actual (blue) and estimated output (red) response of neuronal activity of active channel**

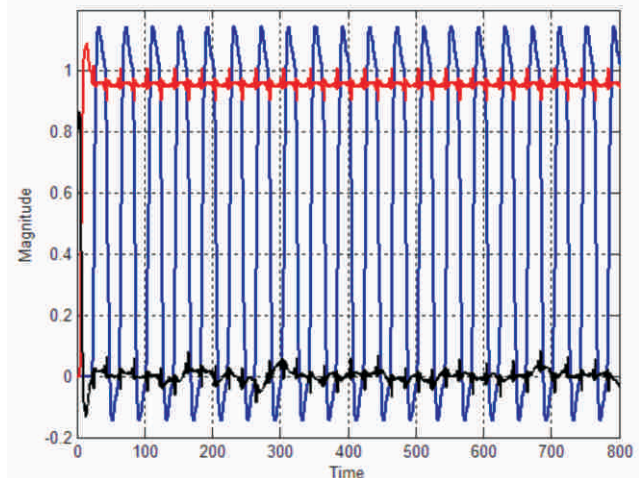


**Figure 5: The actual (blue) and estimated output (red) response of neuronal activity of active channel with error (black) in estimation**

In this study, we have showed that use of delayed version of predicted BOLD response with recursive estimation of unknown parameters can be beneficial in detecting the predicted BOLD response function of active/deactivate channel.

## Acknowledgment

This research was supported by the World Class University program funded by the Ministry of Education, Science and Technology through the National Research Foundation of Korea (grant no. R31-20004).

## References

1. G. Strangman, D. A. Boas, and J. P. Sutton, "Non-invasive neuroimaging using near-infrared light," Society of Biological Psychiatry, vol. 52, 2002, pp. 679-693.

2. F. F. Jobsis, "Noninvasive, infrared monitoring of cerebral and myocardial oxygen sufficiency and circulatory parameters," *Science*, vol. 198, 1977, pp. 1264-1267.
3. Y. Chul, S. Tak, K. E. Jang, J. Jung, and J. Jang, "NIRS-SPM: Statistical parametric mapping for near-infrared spectroscopy," *Neuroimage*, vol. 44, 2009, pp. 428-447.
4. K. Ciftci, B. Sankur, Y. P. Kahya, and A. Akin, "Constructing the general linear model for sensible hemodynamic response function waveform," *Medical & Biological Engineering & Computing*, vol. 46, 2008, pp. 779-787.
5. M. Takeuchi, E. Hori, K. Takamoto, A. H. Tran, K. Satoru, A. Ishikawa, T. Ono, S. Endo, and H. Nishijo, "Brain cortical mapping by simultaneous recording of functional near infrared spectroscopy and electroencephalograms from the whole brain during right median nerve stimulation," *Brain Topography*, vol. 22, 2009, pp. 197-214.
6. G. B. Remijn, M. Kikuchi, Y. Yoshimura, K. Ueno, K. Nagao, T. Munesue, H. Kojima, and Y. Minabe, "Hemodynamic responses to visual stimuli in cortex of adults and 3-to 4-year-old children," *Brain Research*, vol. 1383, 2011, pp. 242-251.
7. A. F. Abdelnour and T. Huppert, "Real-time imaging of human brain function by near infrared spectroscopy using an adaptive general linear model," *Neuroimage*, vol. 46, 2009, pp. 133-143.
8. S. M. Coyle, T. E. Ward, and C. M. Markham, "Brain-computer interface using a simplified functional near-infrared spectroscopy system," *Journal of Neural Engineering*, vol. 4, 2007, pp. 219-226.
9. R. Sitaram, H. Zhang, C. Guan, M. Thulasidas, Y. Hoshi, A. Ishikawa, K. Shimizu, and N. Birbaumer, "Temporal classification of multichannel near-infrared spectroscopy signals of motor imagery for developing a brain-computer interface," *NeuroImage*, vol. 34, 2007, pp. 1416-1427.
10. L. Sheena and T. Chau, "Decoding subjective preference from single-trial near-infrared spectroscopy signals," *Journal of Neural Engineering*, vol. 6, article 016003, 2009.
11. E. Kirilina, A. Jelzow, A. Heine, M. Niessing, H. Wabnitz, R. Brühl, B. Ittermann, A. Jacobs, and I. Tachtsidis, "The physiological origin of task-evoked systemic artefacts in functional near infrared spectroscopy," *Neuroimage*, vol. 61, 2012, pp. 70-81.
12. K. J. Worsley and K. J. Friston, "Analysis of fMRI time-series revisited-again," *Neuroimage*, vol. 2, 1995, pp. 173-181.
13. K. Ciftci, B. Sankur, Y. P. Kahya, and A. Akin, "Multilevel statistical inference from functional near-infrared spectroscopy data during stroop interference," *IEEE Transactions on Biomedical Engineering*, vol. 55, 2008, pp. 2212-2220.
14. S. Haykin, *Adaptive Filtering Theory*, 4th ed., Prentice Hall: New Jersey, 2002, pp. 231-342.
15. M. Aqil, K.-S. Hong, M. Y. Jeong, and S. S. Ge, "Cortical brain imaging by adaptive filtering of NIRS signals," *Neuroscience Letters*, vol. 514, 2012, pp. 35-41.